Journal of Statistical Physics, Vol. 61, Nos. 3/4, 1990

Multifractal Structure of Fully Developed Hydrodynamic Turbulence. II. Intermittency Effects in the Distribution of Passive Scalar Impurities

V. R. Chechetkin,[1] V. S. Lutovinov,[1] and A. Yu. Turygin[1]

Received January 22, 1990; final June 6, 1990

We discuss intermittency effects in the distribution of scalar passive impurities within fully developed hydrodynamic turbulence. It is shown that the observable stronger intermittency effects in the distribution of passive impurities with respect to that for the energy dissipation rate can naturally be explained in the framework of composite random cascade models. We discuss doubly random bounded and unbounded log-normal models, the doubly random β-model, and the two-scale Cantor set approximation. Then the problem of mutual correlations is discussed. The various results are compared with experiments.

KEY WORDS: Intermittency effects in the distribution of passive impurities; composite random cascades; multifractal structure of distribution for passive impurities.

1. INTRODUCTION

The turbulent transport of passive impurities is a fundamental problem in the study of fluid turbulence. It also plays an important role in various practical applications (see, e.g., refs. 1–3). In the case of a steady-state incompressible fluid turbulence, the scaling behavior of the different structure functions for passive impurities is in the first approximation determined by the Obukhov–Corrsin theory.[4,5] However, fluctuations in the local energy transfer rate and turbulent diffusion cause deviations from the Obukhov–Corrsin law called intermittency effects. At first sight the intermittency effects in the distribution of passive impurities should coincide with that of their velocity counterparts, since in the main

[1] Institute of Radioengineering, Electronics and Automation, Moscow, USSR.

0022-4715/90/1100-0589$06.00/0

approximation the general scaling dependences are the same for the turbulent viscous and diffusive dynamics, but it has experimentally been established (see, e.g., refs. 6–9) and references therein) that the intermittency effects in the distribution of passive impurities appear to be stronger than that for the energy dissipation rate. We show in this paper that this experimental fact can naturally be explained in the framework of the composite random cascade models. We consider, in particular, the doubly random β-model and doubly random bounded and unbounded log-normal models. Then we show how the necessary correlations can be taken into account. The results for the various theories are compared and some direct experimental consequences from the composite random nature of cascades are discussed.

2. OBUKHOV–CORRSIN THEORY

For the sake of convenience we reproduce briefly the general outline of the Obukhov–Corrsin theory.[1–5] We restrict ourselves below to the inertial range $L \gg t \gg l_\eta$ (where L and l_η are the external and internal scales of turbulence, respectively). As is well known,[1 3] the effects of molecular diffusivity can be neglected in this range and the turbulent transport in an incomprehensible fluid is given by

$$\frac{\partial \theta}{\partial t} + (\mathbf{v}\Delta)\theta = 0 \tag{1}$$

where $\mathbf{v}(\mathbf{r}, t)$ is a random hydrodynamic velocity and $\theta(\mathbf{r}, t)$ is the concentration of passive impurities. The same equation (1) describes the evolution of temperature disturbances. In what follows the turbulent pulsations of the velocities and concentrations are always understood in the relative sense, $\mathbf{v}(\mathbf{R}+\mathbf{r}, t) - \mathbf{v}(\mathbf{R}, t)$ and $\theta(\mathbf{R}+\mathbf{r}, t) - \theta(\mathbf{R}, t)$.

The consecutive relay turbulent cascade in the inertial range conserves the mean flow,

$$\bar{N} \sim \theta^2(r)/\tau(r) \sim v(r)\,\theta^2(r)/r \tag{2}$$

Using the Kolmogorov expression for the velocity fluctuations[1,2]

$$v(r) \sim \bar{\varepsilon}^{1/3} r^{1/3} \tag{3}$$

where $\bar{\varepsilon}$ is the mean energy dissipation rate per unit mass, one obtains[4,5]

$$\theta(r) \sim \bar{N}^{1/2} r^{1/3} / \bar{\varepsilon}^{1/6} \tag{4}$$

3. β-MODEL

We begin with the simplest approximations and then successively complicate the problem. We first illustrate the general idea of the paper with the use of the homogeneous β-model.[10] It is supposed that the relay turbulent cascade contracts a distribution of passive impurities and the flow N in Eq. (2) curdles in the regions filling only partially the overall physical spece. Let the manifold corresponding to the spatial points where the N flow is not equal to zero form a homogeneous fractal set with Hausdorff dimension $D_{f,N} < D$ (here D is the effective spatial dimension in a physical experiment). Then the balance equation (2) should be replaced by

$$\bar{N} \sim P_{f,N}(r)\, v_{f,N}(r)\, \theta^2_{f,N}(r)/r \tag{5}$$

where $P_{f,N}(r)$ is the probability that an arbitrarily chosen point of a fluid volume with size $\sim r$ $(L > r > l_\eta)$ belongs to the N fractal, and the corresponding subscripts in $v_{f,N}(r)$ and $\theta_{f,N}(r)$ mean that the velocities and concentrations are taken on the N fractal. The probability $P_{f,N}(r)$ has the form

$$P_{f,N}(r) \sim (r/L)^{D - D_{f,N}} \tag{6}$$

On the other hand, the centers of Kolmogorov eddies build up the fractal structure as well.[10] Let $D_{f,\varepsilon} < D$ be its Hausdorff dimension. Then the corresponding balance for the energy transfer rate is given by

$$\bar{\varepsilon} \sim P_{f,\varepsilon}(r)\, v^3_{f,\varepsilon}(r)/r \tag{7}$$

$$P_{f,\varepsilon}(r) \sim (r/L)^{D - D_{f,\varepsilon}} \tag{8}$$

As is seen from Eqs. (1) and (2), the N flow is nonzero only in the spatial regions where $v(r) \neq 0$, i.e., where the ε flow is nonzero. For this reason the probability $P_{f,N}(r)$ can also be presented in the form

$$P_{f,N}(r) = P_{f,\varepsilon}(r)\, P_{f,\varepsilon/N}(r) \tag{9}$$

where $P_{f,\varepsilon}(r)$ is the probability that a point of a fluid volume with size $\sim r$ belongs to ε fractal and $P_{f,\varepsilon/N}(r)$ is the conditional probability that a point of the ε fractal belongs simultaneously to the N fractal. Comparing Eqs. (6), (8) and (9), one obtains

$$P_{f,\varepsilon/N}(r) \sim (r/L)^{D_{f,\varepsilon} - D_{f,N}} \tag{10}$$

This means that the following inequality should hold:

$$D_{f,\varepsilon} \geqslant D_{f,N} \tag{11}$$

i.e., the N fractal should be embedded into the ε fractal (or be a subfractal of the ε fractal). Physically, one can say that the curdling of the N fractal is stronger than that of the ε fractal, or the spatial distribution of the N field is more singular than that of the ε field.

The different moments $\langle N_r^q \rangle$ are determined according to

$$\langle N_r^q \rangle \sim P_{f,N}(r)[v_{f,N}(r)\,\theta_{f,N}^2(r)/r]^q \sim \bar{N}^q P_{f,N}^{1-q}(r) \sim \bar{N}^q (L/r)^{(q-1)(D-D_{f,N})} \tag{12}$$

Defining the exponents $\mu_{q,N}$ by

$$\langle N_r^q \rangle \sim \bar{N}^q (L/r)^{\mu_{q,N}} \tag{13}$$

We obtain from Eqs. (12) and (13) the relationship

$$\mu_{q,N} = (D - D_{f,N})(q-1) \tag{14}$$

The analogous exponents for the ε fluctuations are[10]

$$\mu_{q,\varepsilon} = (D - D_{f,\varepsilon})(q-1) \tag{15}$$

Taking into account Eqs. (11), (14), and (15), one obtains immediately the inequality

$$\mu_{q,N} \geqslant \mu_{q,e} \qquad (q \geqslant 1) \tag{16}$$

i.e., the fluctuations of the N field should be stronger than those of the ε field.

The corresponding moments for the velocities and concentrations are determined by

$$\begin{aligned} \langle v_r^q \rangle &\sim P_{f,\varepsilon}(r)\, v_f^q(r) \\ &\sim \bar{\varepsilon}^{q/3} r^{q/3} (L/r)^{\mu_{q,v}} \\ &\sim \bar{\varepsilon}^{q/3} r^{q/3} (L/r)^{(q/3-1)(D-D_{f,\varepsilon})} \end{aligned} \tag{17a}$$

$$\begin{aligned} \langle \theta_r^q \rangle &\sim \frac{\bar{N}^{q/2}}{\bar{\varepsilon}^{q/6}} r^{q/3} \left(\frac{L}{r}\right)^{\mu_{q,\theta}} \\ &\sim P_{f,N}(r)\, \theta_{f,N}^q(r) \\ &\sim \frac{\bar{N}^{q/2}}{\bar{\varepsilon}^{q/6}} r^{q/3}\, P_{f,N}^{1-q/2}(r)\, P_{f,\varepsilon}^{q/6}(r) \\ &\sim \frac{\bar{N}^{q/2}}{\bar{\varepsilon}^{q/6}} r^{q/3} \left(\frac{L}{r}\right)^{(q/2-1)(D-D_{f,N})-(q/6)(D-D_{f,\varepsilon})} \end{aligned} \tag{17b}$$

This gives that $\mu_{q,\theta} \geqslant \mu_{q,v}$ $(q \geqslant 2)$, i.e., the fluctuations of concentrations should be stronger than those of velocities.

The same suggestions can be generalized to the random β-model.[11] Supposing that the representation of the random curdling factors for the N cascades are in the form of the product of two independent curdling factors analogously to Eq. (9), we can easily obtain for the consecutive contractions of scales at two times that the corresponding exponents $\mu_{q,N}$ defined by Eq. (13) are in this doubly random β-model given by[11]

$$\mu_{q,N} = \log_2 \langle \lambda^{1-q} \rangle + \log_2 \langle \beta^{1-q} \rangle \equiv \mu_{q,\Lambda} + \mu_{q,\varepsilon} \tag{18}$$

$$\langle \beta^{1-q} \rangle = \int_{\beta_{\min}}^{\beta_{\max}} d\beta \, P_\varepsilon(\beta) \beta^{1-q} \tag{19}$$

$$\langle \lambda^{1-q} \rangle = \int_{\lambda_{\min}}^{\lambda_{\max}} d\lambda \, P_\Lambda(\lambda) \lambda^{1-q} \tag{20}$$

$$1 \geqslant \beta_{\max} > \beta_{\min} \geqslant 2^{-D}, \qquad 1 \geqslant \lambda_{\max} > \lambda_{\min} \geqslant 2^{-D} \tag{21}$$

where the probability $P_\varepsilon(\beta)$ describes the distribution of curdling factors for the ε fractals with respect to overall physical space, while the probability $P_\Lambda(\lambda)$ corresponds to the distribution of the relative curdling factors for the N fractals with respect to the ε fractals. It is easy to see that inequality (16) is satisfied in this case as well.

4. LOG-NORMAL MODEL

Experiments[9,12] (see also Fig. 5 in ref. 13) show that in the multifractal picture the inequalities

$$D_q^\varepsilon \geqslant D_q^N \qquad (q \geqslant 0) \tag{22}$$

hold at least up to $q \leqslant 10$. Although the β-model yields the natural explanation of this fact, the above argument is not quite general.

Let us consider the composite representation of N flow in the form

$$N_r = \Lambda_r^{\gamma_\lambda} \varepsilon_r^{\gamma_\varepsilon} \tag{23}$$

with the exponents $\gamma_\lambda > 0$ and $\gamma_\varepsilon > 0$. The multiplicative character of the coupling of N fluctuations with ε fluctuations is rather evident from Eqs. (1) and (2), since the fluctuations in ε_r and the passive nature of turbulent transport should cause the corresponding fluctuations in N_r.

Supposing for simplicity that both Λ_r and ε_r are mutually independent and described by unbounded log-normal distributions with variances $\sigma_\Lambda^2 = \lambda \ln(L/r)$ and $\sigma_\varepsilon^2 = \mu \ln(L/r)$ (cf. refs. 14 and 15; the more general model in the framework of unbounded log-normal distributions has been considered by Van Atta[16]), one obtains

$$\mu_{q,N} = \frac{\lambda}{2} q\gamma_\lambda (q\gamma_\lambda - 1) + \frac{\mu}{2} q\gamma_\varepsilon (q\gamma_\varepsilon - 1) \tag{24}$$

Since the scaling corrections to the mean flow $\langle N_r \rangle$ should be absent, the various parameters are related by the restriction

$$\mu_{1,N} = 0 \tag{25}$$

This condition ensures also the standard multifractal relationship between $\mu_{q,N}$ and D_q^N [see Eq. (33) below]. As can easily be checked, there is a range of parameters where $\lambda > 0$, $\mu > 0$, $\gamma_\lambda > 1$, $0 < \gamma_\varepsilon < 1$, but $\mu_{q,N} < \mu_{q,\varepsilon}$ ($q \geqslant 1$), i.e., the inequalities (22) are violated. On the other hand, the N flow is equal to zero everywhere at all spatial points where the ε flow is equal to zero.

The combination of the inequalities (22) with the composite representation (23) (if possible) may yield interesting physical information related to the internal structure of the N flow and the mutual correlations of ε and N multifractals. We first consider the simplest doubly random cascades

$$N_r = \Lambda_r \varepsilon_r \tag{26}$$

which can be considered as the counterpart of the β-models discussed in the previous section. In the unbounded log-normal model the doubly random representation (26) ensures immediately the inequalities (22) [see Eq. (24)].

In the case of the bounded log-normal model[17] we can use the representation

$$P_N = P_\Lambda P_\varepsilon \tag{27}$$

where each of the probabilities P_Λ and P_ε is described by the equations

$$P(y_r) = A_r \exp\left(- \frac{[\ln(y_r/\bar{y}) + b_r \sigma_r^2]^2}{2\sigma_r^2} \right) \tag{28}$$

$$\langle y_r^q \rangle = \int_{y_{\min,r}}^{y_{\max,r}} dy_r \, P(y_r) \, y_r^q \tag{29}$$

$$\langle y_r^0 \rangle = 1, \qquad \langle y_r \rangle = \bar{y} \tag{30}$$

$$\sigma_r^2 = \mu_r \ln(L/r), \qquad y_{\max,r}/\bar{y} = c_1 (L/r)^{\alpha_1}, \qquad y_{\min,r}/\bar{y} = c_2 (L/r)^{-\alpha_2} \tag{31}$$

with the constants $\alpha_1 > 0$, $\alpha_2 > 0$ and the functions μ_r and b_r weakly dependent on $\ln(L/r)$. As has been argued in ref. 17, a bounded log-normal distribution can be characterized by the triple sets of numbers α_1, α_2, and μ_2.

Having in mind a future application to the experiments by Prasad *et al.*,[9] we describe some results for the case with $\alpha_{1,\Lambda} = 0.115$, $\alpha_{2,\Lambda} = 0.31$, and $\mu_{2,\Lambda} = 0.07$ as a particular example. Figure 1 shows that the asymptotic scaling behaviors for the moments $\langle \Lambda_r^q \rangle$ are fulfilled with a good accuracy despite the relative smallness of the logarithmic range in the corresponding integrals (29). Taking the values $\alpha_{1,\varepsilon} = 0.485$, $\alpha_{2,\varepsilon} = 0.74$, and $\mu_{2,\varepsilon} = 0.25$ for the distribution of ε fluctuations, we present also the results for C_q^N and μ_q (see Figs. 2 and 3) determined by

$$\langle N_r^q \rangle = C_q^N (L/r)^{\mu_{q,N}} = C_q^\Lambda C_q^\varepsilon (L/r)^{\mu_{q,\Lambda} + \mu_{q,\varepsilon}} \tag{32}$$

(the corresponding plots for C_q^ε and $\mu_{q,\varepsilon}$ are given in Figs. 4 and 5 in ref. 17).

In order to describe the statistical characteristics of fluctuations in terms of the generalized Renyi dimensions, it is useful to define them for the factorized Λ–ε model (26) according to

$$\mu_{q,N} = (D - D_q^N)(q-1), \qquad \mu_{q,\varepsilon} = (D - D_q^\varepsilon)(q-1), \qquad \mu_{q,\Lambda} = D_q^\Lambda (q-1) \tag{33}$$

Then the equality

$$\mu_{q,N} = \mu_{q,\Lambda} + \mu_{q,\varepsilon} \tag{34}$$

gives

$$D_q^\Lambda = D_q^\varepsilon - D_q^N \tag{35}$$

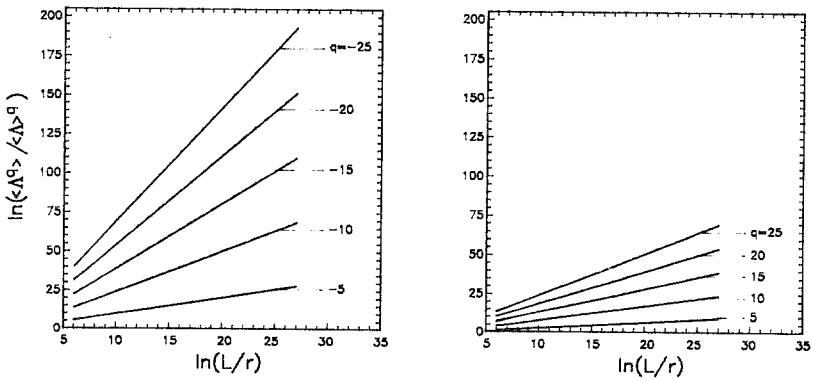

Fig. 1. The asymptotic scaling behavior of moments $\langle \Lambda_r^q \rangle$ for the bounded log-normal distribution with $\alpha_{1,\Lambda} = 0.115$, $\alpha_{2,\Lambda} = 0.31$, and $\mu_{2,\Lambda} = 0.07$.

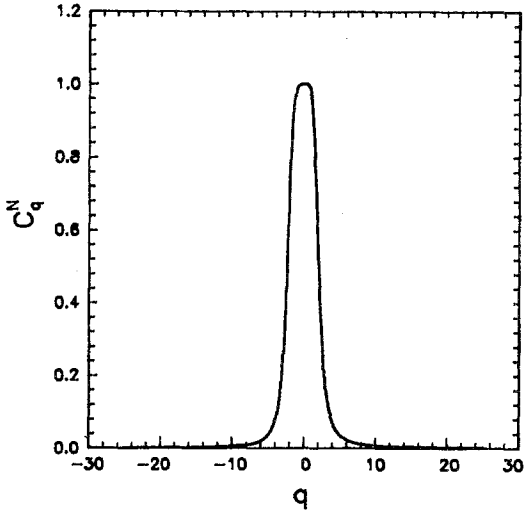

Fig. 2. The constant C_q^N versus q for the factorized distribution (27) with the product of two bounded log-normal probabilities with parameters $\alpha_{1,A}=0.115$, $\alpha_{2,A}=0.31$, $\mu_{2,A}=0.07$ and $\alpha_{1,\varepsilon}=0.485$, $\alpha_{2,\varepsilon}=0.74$, $\mu_{2,\varepsilon}=0.25$, respectively [see Eq. (32)].

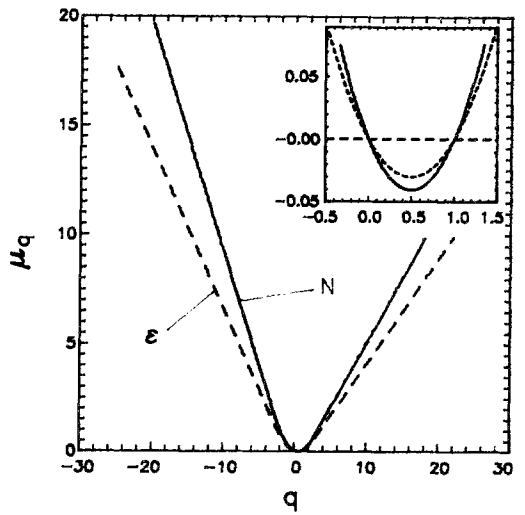

Fig. 3. The exponent μ_q versus q in the case of ε fluctuations (dashed line) for the bounded log-normal distribution with $\alpha_{1,\varepsilon}=0.485$, $\alpha_{2,\varepsilon}=0.74$, and $\mu_{2,\varepsilon}=0.25$ and in the case of N fluctuations (solid line) for the same factorized distribution as in Fig. 2.

Analogously to the case of ε fluctuations,[12] the experimental data for the one-dimensional cuts ($D=1$) of N fluctuations[9] can empirically be described with an accuracy $\sim 10\%$ by the two-scale Cantor set dimensions,

$$D_q^N = \frac{1}{(1-q)} \log_2(0.76^q + 0.24^q) \tag{36}$$

The fit for the doubly random β-model [see Eqs. (18)–(21)] is performed as in refs. 11 and 17 and gives the exponents

$$\begin{aligned} \mu_{q,N} &= \log_2[0.6 \times 2^{-0.115(1-q)} + 0.4] \\ &\quad + \log_2[0.47 \times 2^{-0.485(1-q)} + 0.53] \\ &\equiv \mu_{q,\Lambda} + \mu_{q,\varepsilon} \end{aligned} \tag{37}$$

Figures 4 and 5 summarize the results for various theories. Although the agreement between the experimental data and the doubly random β-model can be improved for positive $q>0$ by a more flexible choice of probabilities $P_\Lambda(\lambda)$ and $P_\varepsilon(\beta)$ in Eqs. (18)–(21), the principal inequality $D \geqslant D_{-\infty}^N$ breaks the correspondence for negative values of $q<0$ (see Fig. 4).

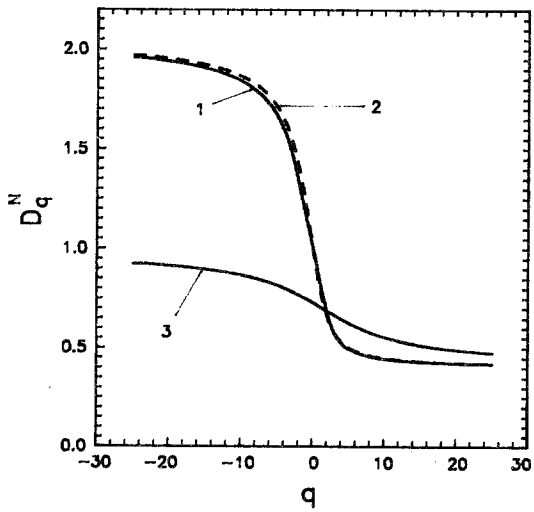

Fig. 4. The generalized Renyi dimension D_q versus q for various models of intermittency. (1) The factorized Λ–ε model (26) with the product of two bounded log-normal distributions with parameters $\alpha_{1,\Lambda}=0.115$, $\alpha_{2,\Lambda}=0.31$, $\mu_{2,\Lambda}=0.07$ and $\alpha_{1,\varepsilon}=0.485$, $\alpha_{2,\varepsilon}=0.74$, $\mu_{2,\varepsilon}=0.25$ (solid line); (2) two-scale Cantor set approximation (36) (dashed line); (3) doubly random β-model (37).

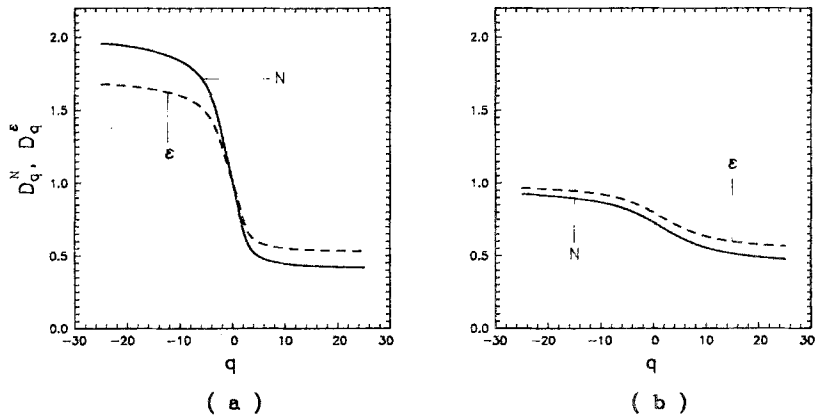

Fig. 5. The generalized Renyi dimension D_q versus q for the ε fluctuations (dashed lines) and for the N fluctuations (solid lines) in the case of (a) the factorized Λ–ε model with the product of two bounded log-normal distributions with the same parameters as in Fig. 4 and (b) in the case of random and doubly random β-models [see Eq. (37)].

Moreover, the mutual relationships for the ε and N fluctuations cannot even qualitatively be satisfied in the random β-models for $q < 0$ (see Fig. 5).

The more singular spatial distribution of the N field and the stronger character of concentration fluctuations may be described not only in terms of inequalities, $D_q^\varepsilon \geqslant D_q^N$ $(q \geqslant 0)$ and $\mu_q^N \geqslant \mu_q^\varepsilon$ $(q \geqslant 1)$, but also with the use of the so-called f–α curves[18–20] determined parametrically by

$$(q-1)D_q = q\alpha(q) - f(\alpha(q)) \tag{38}$$

$$\alpha(q) = \frac{d}{dq}[(q-1)D_q] \tag{39}$$

The function $f(\alpha)$ characterizes the fractal dimensions of spatial regions, where the local fields behave as $(r/L)^{\alpha - D}$ at $r \ll L$ (a more general definition can be found in ref. 21). The comparative f–α curves for the ε and N fluctuations are shown in Fig. 6. It is worth noting that f–α curves also can be directly measured experimentally.[22–25]

The composite nature of N cascades in the representation (26) can be expressed in terms of the inequality

$$D_{q2}^\varepsilon - D_{q2}^N \geqslant D_{q1}^\varepsilon - D_{q1}^N \qquad (q_2 \geqslant q_1 \geqslant 0) \tag{40}$$

since the relative generalized dimensions D_q^Λ in Eq. (35) increase with increasing q [their behavior is analogous to that of $(D - D_q^\varepsilon)$ or $(D - D_q^N)$ with D_q^ε and D_q^N decreasing with increase of q (see Fig. 5)]. The restriction (40) is more severe than inequality (22).

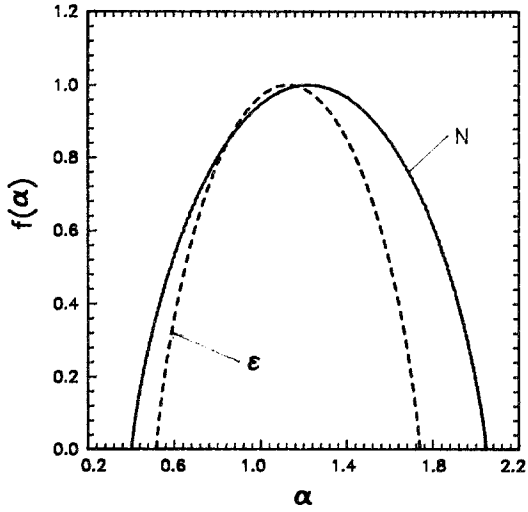

Fig. 6. The f–α curves for ε fluctuations (dashed line) and for N fluctuations (solid line) in the case of two-scale Cantor set approximations.

5. CORRELATED Λ–ϵ MODEL. CONCLUSION

The representation (23) corresponds to the following physical situation. It is supposed that a part of the renormalized turbulent diffusive dynamics lags from the initial dynamics of ε flow and becomes more or less independent of ε. This is due to the causality principle and the fact that the renormalized turbulent diffusion dynamics is determined by the retarded velocity correlators. The superimposition of the lagging and initial dynamics is simulated by the composite representation (23). The doubly random approximation oversimplifies this process and generally Λ_r and ε_r should partially be correlated. For definiteness we restrict ourselves to the bounded log-normal distributions.

The direct generalization of the Van Atta[16] model to Λ–ε correlations in the form (26) is impossible, since Λ–ε correlations would immediately cause unphysical scaling corrections to the averaged flow $\langle N_r \rangle$ [cf. Eq. (25)]. One way to overcome this difficulty consists in the more complicated composite representation for the variable Λ_r:

$$\Lambda_r = \prod_{j=1}^{m} \Lambda_{jr} \tag{41}$$

where the mutual correlations of the random variables Λ_{jr} and ε_r are

introduced analogously to the Van Atta[16] model and are restricted by the condition

$$\langle N_r \rangle = \bar{N} \tag{42}$$

The various free parameters are then fitted with respect to the experimental data.

One could, however, use the fact that Λ_r is a hidden auxiliary variable and replace Eq. (26) by

$$N_r = \Lambda_r^{\gamma} \varepsilon_r \tag{43}$$

with the correlated Λ–ε parts and the exponent γ fixed by Eq. (25). From a pragmatic point of view such a representation is more convenient for comparison with experiment, since the number of fitting parameters is much less. The choice of the form $\Lambda_r^{\gamma}\varepsilon_r$ rather than $\Lambda_r \varepsilon_r^{\gamma}$ is again dictated by inequality (22). The mutual probability distribution function is assumed to be of the form[16,25]

$$\begin{aligned} \Pi(\Lambda_r, \varepsilon_r) = \frac{\Lambda_r}{\Lambda_r \varepsilon_r} \exp \left\{ -\frac{1}{(1-\rho_{\varepsilon-\Lambda}^2)} \left[\frac{[\ln(\Lambda_r/\bar{\Lambda}) + b_\Lambda \sigma_{\Lambda,r}^2]^2}{2\sigma_{\Lambda,r}^2} \right.\right. \\ - \rho_{\varepsilon-\Lambda} \frac{[\ln(\Lambda_r/\bar{\Lambda}) + b_\Lambda \sigma_{\Lambda,r}^2][\ln(\varepsilon_r/\bar{\varepsilon}) + b_\varepsilon \sigma_{\varepsilon,r}^2]}{\sigma_{\Lambda,r}\sigma_{\varepsilon,r}} \\ \left.\left. + \frac{[\ln(\varepsilon_r/\bar{\varepsilon}) + b_\varepsilon \sigma_{\varepsilon,r}^2]^2}{2\sigma_{\varepsilon,r}^2} \right] \right\} \end{aligned} \tag{44}$$

The limits of integration and other parameters are determined analogously to Eqs. (28)–(31).

The mutual correlations are characterized by the cross-exponents $M(q, p)$ defined by the moments

$$\langle \varepsilon_r^q N_r^p \rangle \propto \bar{\varepsilon}^q \bar{N}^p (L/r)^{M_{\varepsilon-N}(q,p)} \tag{45}$$

$$\langle \varepsilon_r^q \Lambda_r^p \rangle \propto \bar{\varepsilon}^q \bar{\Lambda}^p (L/r)^{M_{\varepsilon-\Lambda}(q,p)} \tag{46}$$

$$M_{\varepsilon-N}(q, p) = M_{\varepsilon-\Lambda}(q+p, \gamma p) \tag{47}$$

The exponents $M(q, p)$ are related to $\tau(q, p)$ used in ref. 25 by

$$M(q, p) = (q+p-1)D - \tau(q, p) \tag{48}$$

The fitting parameters in Eqs. (43) and (44) are determined by the relatively low values of q and p [see Eqs. (50) below]. For this reason we illustrate the fitting procedure using the unbounded cross-exponents[8,16,25]:

$$M_{\varepsilon-\Lambda}(q, p) \approx \frac{\mu_\varepsilon q(q-1)}{2} + \frac{\mu_\Lambda p(p-1)}{2} + \rho_{\varepsilon-\Lambda} qp(\mu_\varepsilon \mu_\Lambda)^{1/2} \tag{49}$$

where the fitting parameters in Eqs. (43)–(47) are determined by the conditions

$$M_{\varepsilon\text{-}N}(2,0)=\mu_{2,\varepsilon};\qquad M_{\varepsilon\text{-}N}(0,2)=\mu_{2,N} \tag{50a}$$

$$M_{\varepsilon\text{-}N}(1,1)=\rho_{\varepsilon\text{-}N}(\mu_{2,\varepsilon}\mu_{2,N})^{1/2} \tag{50b}$$

$$M_{\varepsilon\text{-}N}(1,0)=0;\qquad M_{\varepsilon\text{-}N}(0,1)=0 \tag{50c}$$

with the known experimental values on the rhs of Eqs. (50). This gives ($\mu_\varepsilon \approx \mu_{2,\varepsilon}$, $\mu_N \approx \mu_{2,N}$)

$$\gamma = 1+\frac{2[\mu_\varepsilon-\rho_{\varepsilon\text{-}N}(\mu_\varepsilon\mu_N)^{1/2}]}{\mu_N-\mu_\varepsilon} \tag{51}$$

$$\mu_A=(\mu_N-\mu_\varepsilon)/\gamma \tag{52}$$

$$\rho_{\varepsilon\text{-}A}=\frac{1-\gamma}{2}\left(\frac{\mu_A}{\mu_\varepsilon}\right)^{1/2} \tag{53}$$

while the boundary exponents [see Eq. (31)] are determined by

$$\alpha_{1,\varepsilon}=D-D^{\varepsilon}_{\infty};\qquad \alpha_{2,\varepsilon}=D^{\varepsilon}_{-\infty}-D \tag{54}$$

$$\alpha_{1,A}=(D^{\varepsilon}_{\infty}-D^{N}_{\infty})/\gamma;\qquad \alpha_{2,A}=(D^{N}_{-\infty}-D^{\varepsilon}_{-\infty})/\gamma \tag{55}$$

We should, however, especially stress that the expressions (49) and (51)–(53) are valid only for the unbounded correlated log-normal distributions and in the bounded model they can be used only for approximate preliminary estimates. Even if the relatively weak dependences on $\ln(L/r)$ in $b_{A,r}$, $\mu_{A,r}$, $b_{\varepsilon,r}$, $\mu_{\varepsilon,r}$, and $\rho_{\varepsilon\text{-}A,r}$ are neglected (cf. ref. 17 and Section 4), their values must be fitted numerically by the conditions (50) and may generally be different from the estimates given by Eqs. (49), and (51)–(53). Thus, the unbounded estimates should at least be numerically checked by the fulfilment of conditions (50). Our calculations show that they are not always satisfactory.

If $\rho_{\varepsilon\text{-}A}$ is equal to zero, then this model is reduced to the doubly random representation (26) and (27). Both models describe D^N_q curves equally well, but their dependences on the ε–N mutual correlations are different. For the doubly random model (26), $\rho_{\varepsilon\text{-}N}$ cannot be considered as an independent experimental parameter and one obtains $\rho_{\varepsilon\text{-}N}\approx(\mu_\varepsilon/\mu_N)^{1/2}$ [cf. Eq. (51)]. This difference would show up both in the cross-moments (45) and in the weighted concentration averages [see Eq. (4)]:

$$\langle\theta^q_r\rangle \sim \left\langle\frac{N^{q/2}_r r^{q/3}}{\varepsilon^{q/6}_r}\right\rangle \sim \frac{\bar{N}^{q/2}}{\bar{\varepsilon}^{q/6}} r^{q/3}\left(\frac{L}{r}\right)^{M_{\varepsilon\text{-}N}(-q/6,q/2)} \tag{56}$$

The corresponding plots for the exponent

$$\zeta_q = q/3 - M_{\varepsilon-N}(-q/6, q/2) = q/3 - M_{\varepsilon-\Lambda}(q/3, \gamma q/2) \tag{57}$$

are shown in Fig. 7. The dot-dashed curve 3 corresponds to the doubly random, bounded log-normal representation (26), (27) with the same parameters as used in Section 4 (see also Fig. 4). This curve appears to be in a rather good correlation with the experimental data of ref. 8. Curves 1 and 2 illustrate the influence of the mutual correlations in the Λ^γ–ε model (43). The solid curve 1 reproduces reasonably well the data of ref. 25.

Below we give a brief discussion of the experimental situation and other problems. The criterion for the composite representation of the N flow in the form (43) is also expressed by inequality (40). The experimental data[9,25] (see also Fig. 5 in ref. 13) support this idea at least up to $q \leqslant 10$. The results for the higher moments are more ambiguous. In refs. 9 and 12 it has, in particular, been obtained that $\mu_2^N = 0.38 \pm 0.08$ and $\mu_2^\varepsilon = 0.25 \pm 0.05$ (or $D_2^N = 0.62 \pm 0.08$ and $D_2^\varepsilon = 0.75 \pm 0.05$), while $D_\infty^N \approx 0.40 \pm 0.10$ and $D_\infty^\varepsilon \approx 0.51 \pm 0.10$. We have chosen in our calculations the values $\mu_2^N = 0.32$, $D_\infty^N = 0.4$ and $\mu_2^\varepsilon = 0.25$, $D_\infty^\varepsilon = 0.51$, which lie within the experimental errors. However, the change of $\mu_2^N = 0.32$ to $\mu_2^N = 0.38$ would

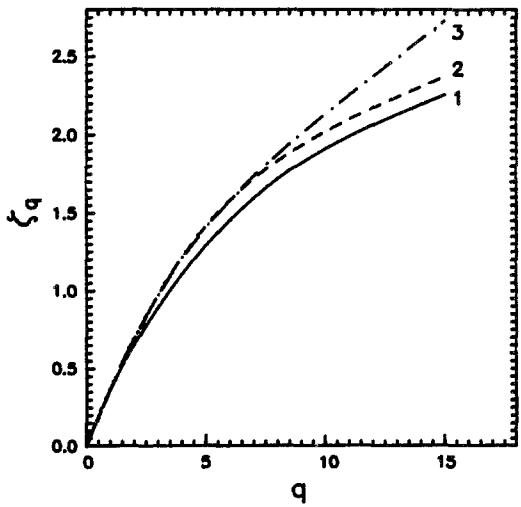

Fig. 7. The exponent ζ_q [see Eq. (57)] versus q. (1) Solid line: the correlated Λ^γ–ε model (43) with $\alpha_{1,\Lambda} = 0.033$, $\alpha_{2,\Lambda} = 0.044$, $\mu_{r,\Lambda} = 0.095$, $\gamma = 7.0$, and $\rho_{\varepsilon-\Lambda} = -0.5$ (or $\rho_{\varepsilon-N} = 0.39$); (2) dashed line: $\alpha_{1,\Lambda} = 0.23$, $\alpha_{2,\Lambda} = 0.31$, $\mu_{r,\Lambda} = 0.047$, $\gamma = 1$, and $\rho_{\varepsilon-\Lambda} = 0$ (or $\rho_{\varepsilon-N} = 0.95$); (3) dot-dashed line: $\alpha_{1,\Lambda} = 0.115$, $\alpha_{2,\Lambda} = 0.31$, $\mu_{r,\Lambda} = 0.095$, $\gamma = 1$, and $\rho_{\varepsilon-\Lambda} = 0$ (or $\rho_{\varepsilon-N} = 0.94$). In all cases $\alpha_{1,\varepsilon} = 0.485$, $\alpha_{2,\varepsilon} = 0.74$, and $\mu_{r,\varepsilon} = 0.25$. These parameters (for all curves) correspond to $\mu_{2,N} = 0.32$ and $\mu_{2,\varepsilon} = 0.25$.

cause the violation of the criterion (40) and rule out the composite nature of the N cascades. The recent estimate $D^{\varepsilon}_{\infty} = 0.12 \pm 0.08$ suggested by Meneveau and Sreenivasan[24] makes the situation even more confused.

If the inequalities (22) are fulfilled but the criterion (40) is violated, then N flow should be treated as a unit indispersible process. In the last case D^{N}_{q} could be described by the corresponding nonfactorized, bounded log-normal distribution[17] with the ε–N correlations introduced by analogy with ref. 16 (see also ref. 25), i.e., one should use the direct mutual probability $\Pi(\varepsilon_r, N_r)$ analogously to Eq. (44) rather than composite representations of the type of (23). It is worth noting that the generalized Renyi dimensions for the nonfactorized, bounded log-normal distribution (28)–(31) with the parameters $\alpha_1 = \alpha_{1,\Lambda} + \alpha_{1,\varepsilon}$, $\alpha_2 = \alpha_{2,\Lambda} + \alpha_{2,\varepsilon}$, and $\mu_2 = \mu_{2,\Lambda} + \mu_{2,\varepsilon}$ would practically merge with the corresponding curve for the factorized distribution (27) in Fig. 4 (even closer than the dashed line in this figure). Thus, the criterion (40) is really essential from the experimental point of view.

The mutual ε–N correlations have been studied extensively in ref. 25. These authors investigated the surrogate flows

$$N' \propto (\partial T/\partial t)^2, \qquad \varepsilon' \propto (\partial v/\partial t)^2 \tag{58}$$

and found very low correlation coefficient $\rho_{\varepsilon'-N'} = 0.13$. The value $\rho_{\varepsilon-N} = 0.3$ obtained from the temperature structure functions is probably more adequate, since the intermittency effects in the temperature structure functions are determined by the real ε and N flows rather than ε' and N'. The other specific feature of these experiments is the strong anisotropy of the turbulence. The correlation for ε' and the squared vorticity,

$$\omega_r^2 = [\text{rot } \mathbf{v}(\mathbf{r}, t)]^2$$

was found to be equal to $\rho_{\varepsilon'-\omega_r^2} = 0.3$, while for isotropic conditions this value should be expected to be close to unity, since

$$\overline{(\text{rot } \mathbf{v})^2} = \varepsilon/\nu$$

where the bar means the averaging over the solid angle and ν is the molecular viscosity (see, e.g., ref. 2). The early value $\rho_{\varepsilon-N} = 0.5$ reported in refs. 26 and 27, interpreted within the framework of the composite representation, might indicate a relatively low correlation of Λ–ε parts because the value 0.5 does not strongly differ from the value $\rho_{\varepsilon-N} = (\mu_\varepsilon/\mu_N)^{1/2}$ obtained in the doubly random N cascades. All experiments give, however, unambiguous evidence on the necessity of Λ–ε correlations [if criterion (40) is fulfilled].

It is worth noting that the composite representation for N flow (if possible) is more informative than the ε–N correlations in the form of ref. 16, since it sheds additional light on the internal structure of N cascades. Thus, despite the evident phenomenology, such a composite representation may appear useful in future investigations.

Finally, we note that inequalities analogous to (22) can also be written for the moments of the high-order spatial derivatives of the same quantity, since a spatial differentiation is a contraction operation. It gives immediately the restriction

$$D_q^{(m)} \geqslant D_q^{(n)} \qquad (m \leqslant n,\ q \geqslant 0) \tag{59}$$

where m and n correspond to the orders of the differentiation. For this reason the distributions of the higher derivatives should be more singular than that of the lower ones, while their f–α curves should encompass the corresponding f–α curves of the lower derivatives (cf. Figs. 5a and 6). This conclusion is in good agreement with the experimental observations on the moments of the spatial derivatives of the velocities.[28] It is of interest to check whether a stronger restriction analogous to Eq. (37) does or does not hold in this case and to investigate also the moments of the spatial derivatives of the temperature or concentration.

ACKNOWLEDGMENTS

The authors thank to A. A. Vedenov and A. L. Chernjakov for helpful discussions and remarks. We are also indebted to Dr. K. R. Sreenivasan and Editorial Staff for information on refs. 24 and 25.

REFERENCES

1. A. S. Monin and A. M. Yaglom, *Statistical Fluid Mechanics*, Vol. II (MIT, Cambridge, 1975).
2. L. D. Landau and E. M. Lifshitz, *Fluid Mechanics*, 2nd ed. (Pergamon Press, 1987).
3. G. T. Csanady, *Turbulent Diffusion in the Environment* (D. Reidel, Dordrecht, 1973).
4. A. M. Obukhov, *Izv. Akad. Nauk SSSR Geograf. Geofiz.* **13**:58 (1949).
5. S. Corrsin, *J. Appl. Phys.* **22**:469 (1951).
6. R. M. Williams and C. A. Paulson, *J. Fluid Mech.* **83**:547 (1977).
7. K. R. Sreenivasan, R. A. Antonia, and H. Q. Dahn, *Phys. Fluids* **20**:1238 (1977).
8. R. A. Antonia, E. J. Hopfinger, Y. Gagne, and F. Anselmet, *Phys. Rev. A* **30**:2704 (1984).
9. R. R. Prasad, C. Meneveau, and K. R. Sreenivasan, *Phys. Rev. Lett.* **61**:74 (1988).
10. U. Frisch, P.-L. Sulem, and M. Nelkin, *J. Fluid Mech.* **87**:719 (1978).
11. R. Benzi, G. Paladin, G. Parisi, and A. Vulpiani, *J. Phys. A* **17**:3521 (1984).
12. C. Meneveau and K. R. Sreenivasan, *Phys. Rev. Lett.* **59**:1424 (1987).
13. K. R. Sreenivasan and R. R. Prasad, *Physica D* **38**:322 (1989).
14. A. M. Obukhov, *J. Fluid Mech.* **13**:77 (1962).

15. A. N. Kolmogorov, *J. Fluid Mech.* **13**:82 (1962).
16. C. W. Van Atta, *Phys. Fluids* **14**:1803 (1971).
17. V. R. Chechetkin, V. S. Lutovinov, and A. Yu. Turygin, *J. Stat. Phys.*, this issue, preceding paper.
18. H. G. Hentschel and I. Procaccia, *Physica D* **8**:435 (1983).
19. P. Grassberger, *Phys. Lett. A* **97**:227 (1983); **107**:101 (1985).
20. T. C. Halsey, M. H. Jensen, L. P. Kadanoff, I. Procaccia, and B. I. Shraiman, *Phys. Rev. B* **33**:1141 (1986).
21. B. B. Mandelbrot, in *Random Fluctuations and Pattern Growth: Experiments and Models*, H. E. Stanley and N. Ostrowsky, eds. (Kluwer, Dordrecht, 1988), pp. 279–291.
22. A. Chhabra and R. V. Jensen, *Phys. Rev. Lett.* **62**:1327 (1989).
23. A. Chhabra, C. Meneveau, R. V. Jensen, and K. R. Sreenivasan, *Phys. Rev. A* **40**:5284 (1989).
24. C. Meneveau and K. R. Sreenivasan, *J. Fluid Mech.* (in press).
25. C. Meneveau, K. R. Sreenivasan, P. Kailasnath, and M. S. Fan, *Phys. Rev. A* **41**:894 (1990).
26. R. A. Antonia and C. W. Van Atta, *J. Fluid Mech.* **67**:273 (1975).
27. R. A. Antonia and A. J. Chambers, *Boundary-Layer Meteorol.* **18**:399 (1980).
28. K. R. Sreenivasan and C. Meneveau, *Phys. Rev. A* **38**:6287 (1988).